pp. 29:34

The Identification of the Modal Parameters of Orbital Machines using Dynamic Structural Approach

Hossein Pirzadeh, Alireza Mohammadion*, Armen Adamian

Department of Mechanical Engineering, Central Tehran Branch, Islamic Azad University, Tehran, Iran,
hpirzadeh@hotmail.com, ar.mohammadion@gmail.com, arm.adamian@iauctb.ac.ir

Abstract

The researcher measured the least number of frequency response functions required for the identification of modal parameters, in order to simplify the identification of modal properties of such systems. In this work, the orbital machines are supposed to be a combination of orbital and non-orbital components. Structural Approach specified the identification of dynamic properties only to those phrases that contain responses to a driving force. It has been revealed that the identification of dynamic properties distinguishes the orbital and non-orbital components of the structures and as a result, non-symmetric sections of the space coordinate matrixes become obvious. The application of the above approach was examined on two different structures. The first examination was on a computer-simulated rotor model with four degrees of freedom. In this case, the theoretical properties of this approach were evaluated, while the noise factor was disregarded. The second examination was done on a true machine, whereby the probable problems of the implementation of the suggested approach were clarified. The complete modal identification of an orbital system takes place without the need to measure a complete row of FRF matrixes. The number of the elements to be measured in an FRF matrix depends on the number of degrees of freedom of the system and on the non-symmetric sections of the stuffiness and damping matrixes. The number of elements of the left specific axis that should be measured directly from the evaluated data depends on the matrix sub-ranks, which is composed of non-symmetric sections of space-featured matrixes.

Keywords: Modal parameters, orbital machines, FRF matrixes, degree of freedom, dynamic properties
Article history: Received 22-APR-2018; Revised 10-MAY-2018; Accepted 02-JUN-2018.

1. Introduction

In the case of industrial machines, measurement and vibration monitoring are remarkably of high importance, because malfunctioning in any of these two factors causes great destructive effects in this area. Selection of the type of vibration sensor in accordance with its utilization has a direct effect on the accuracy and scrutiny of the vibration measurement. The act of vibration measurement should be done via manual analyzers and in places without vibration sensors in order to prevent or repair the possible disorders in vibration monitoring or its accuracy. Identification of the malfunctioning in orbital machines was done by using different markers. Generally, condition monitoring could be investigated through four categories, namely Electrical parameters, Chemical parameters, Thermal monitoring, and Mechanical parameters. The common problems of electrical orbital motors stem from their dependence on offset situation and lack of balance in the motors themselves, whereby the vibration analysis would be of a great help.[1], [2] The scope of overall vibration amplitude of machines is a good clue for solving the problems in most of the cases, but as Mortazavie et al. [3] claimed, it is not applicable and suitable in all of the cases and for all types of the problems. Poihnen [4] showed that the electromagnetic force is the most sensitive marker of error condition in the offset in aerial distances; hence, there are identifiable clues in the vibration patterns of machines. The only weakness of this clue is its inaccessibility. As far as vibration is because of the mutual effects of the forces on the structure of the machine, most of the bearing failures diagnosis depend upon the vibration analysis methods such as Hilbert & Wavelet transform or stream analysis. Choi et al.[5] discovered that how the analysis of vibration enables the offset diagnosis too. Measuring the total number of vibrations in a frequency spectrum for an effective frequency range (from dc range to the possible favourite frequency) is viable through different methods, one of which was provided by Durrel et al.[6] previously. The most common method of vibration analysis in the industrial units is the analysis in time domain. Finlay et al.[7] provided a list of mechanical and electrical problems that are identifiable by frequency components of vibration patterns. This analytical approach was based on wandering waves, Zhug[8] where magnetic flux waves in aerial distance are investigated as the result of action and the driving force. Measurement and analysis of the vocal noise spectrum is another method of diagnosis in electrical orbital machines, which has its own requirements and necessities. The vocal noise emitted from aerial distance can be an indication of the probable offset in faradic motors, but its measurement is not that valuable in noisy places i.e. a factory. Cameron[9] evaluated the success of vocal noise analysis approach in combination with Wigner–Ville distribution in order to diagnose the gearbox problems. In the reference number [10] it was shown that how a machine's future life could be estimated via extracting information about vocal noise signals. Rodríguez[11] explained that problems with the components of Roller Bearing result in provocation of specific frequencies that can be identified in acoustic spectrum. In Rodriguez's work, an automatic method diagnoses the problems and by using vocal signal noises emitted from the orbital machines determines their remained life. Comparing the estimated torque and the measured torque, identification of some of the problems in electrical orbital machines becomes possible. Hence, it is necessary for this approach to have an acceptable model and algorithm in order to be aware of real torque aerial distance. In Lee et al.[12], torque estimation and tensional vibration analysis were used for diagnosing the gearbox in a traction system, which showed agreement with its measured torque. Guzinski et al.[13] used torque inspector without any extra sensor for diagnosing the problems in transportation system and high-speed trains. The inspector was able to identify the frequencies of test table network, which had small amplitude in an intact gearbox.

Usually, dynamic properties of dynamic systems are described in three dependent approaches: Modal model, Spatial model, and Response model. The most common approach for showing dynamic properties in a structure is the one that is based on the dominant moods. Accordingly, in a specific scope of frequencies, a machine's performance can be supposed as a system with some limited degrees of freedom. This supposition enables us to describe modal parameters of a structure in the form of matrixes with fixed and limited sizes.

2. Modal Parameters

As Stuffiness and Damping matrixes are not symmetric, modal model of orbital machines structure include two different sets of modal axis i.e. specific left axis and specific right axis with some special sizes and values. As it is clear, this model differs from non-orbital structures that were previously discussed, which were made up of only right-specific axis and special sizes and values.

In the structure of orbital machines, the specific right amounts and specific axis are calculated thorough the symmetric section of below equation [14]:

$$\left[i\omega \cdot \begin{bmatrix} [0] & [M] \\ [M] & [C] \end{bmatrix} + \begin{bmatrix} -[M] & [0] \\ [0] & [K] \end{bmatrix} \right] \begin{Bmatrix} i\omega \cdot \{X(\omega)\} \\ \{X(\omega)\} \end{Bmatrix} = \begin{Bmatrix} \{0\} \\ \{F(\omega)\} \end{Bmatrix} \quad (1)$$

This is as:

$$\left[\begin{bmatrix} [0] & [M] \\ [M] & [C] \end{bmatrix} \cdot \lambda_r + \begin{bmatrix} -[M] & [0] \\ [0] & [K] \end{bmatrix} \right] \begin{Bmatrix} \{\Psi_R\}_r \cdot \lambda_r \\ \{\Psi_R\}_r \end{Bmatrix} = \begin{Bmatrix} \{0\} \\ \{0\} \end{Bmatrix} \quad (2)$$

In this relationship $\{\Psi_R\}_r$ is the right specific axis and λ_r is the r mode.

The left specific axis is calculated as below:

$$\left[\begin{bmatrix} [0] & [M] \\ [M] & [C] \end{bmatrix}^T \cdot \lambda_r + \begin{bmatrix} -[M] & [0] \\ [0] & [K] \end{bmatrix}^T \right] \begin{Bmatrix} \{\Psi_L\}_r \cdot \lambda_r \\ \{\Psi_L\}_r \end{Bmatrix} = \begin{Bmatrix} \{0\} \\ \{0\} \end{Bmatrix} \quad (3)$$

In this relation $\{\Psi_L\}_r$ is the specific left axis.

For a system in N rank, the number of the moods is 2N, each of which has its own specific amount in specific left and specific right axis. If Mass, Stuffiness and Damping Matrixes are real, then specific right axis, specific left axis, and specific amounts appear as N Complex Conjugate pairs. In this condition, specific amounts, specific right and specific left matrixes related to situation space $\{\tilde{\Psi}_L\}$, $\{\tilde{\Psi}_R\}$ and $\{\tilde{\lambda}\}$ have the overall format as below:

$$\underset{2N\times 2N}{[\tilde{\lambda}]} = \begin{bmatrix} [\lambda]^* & [0] \\ [0] & [\lambda] \end{bmatrix} \quad (4)$$

$$\underset{2N\times 2N}{[\tilde{\Psi}_R]} = \begin{bmatrix} [\Psi_R]^*[\lambda]^* & [\Psi_R][\lambda] \\ [\Psi_R]^* & [\Psi_R] \end{bmatrix} \quad (5)$$

$$\underset{2N\times 2N}{[\tilde{\Psi}_L]} = \begin{bmatrix} [\Psi_L]^*[\lambda]^* & [\Psi_L][\lambda] \\ [\Psi_L]^* & [\Psi_L] \end{bmatrix} \quad (6)$$

As in non-orbital machines, the specific amounts and specific right axis in orbital machine structures are indicators of free vibrations, whereby specific right axis components stand for the amplitude and phase of movement in every degree of freedom, and also, specific amounts show the frequencies and their damping rates. The exact physical interpretation of specific amounts and specific axis could be fulfilled via system movement equations.

3. Instruments and Methodology

The content of this research deals with application of descriptive approach. In precise, this approach is referred to as “Prediction Approach”, because instead of the direct extraction of the specific left axis from measurements, it aims at estimating them.

At first, a numerical model relevant to a system with four degrees of freedom is studied. The beginning point for describing a rotator is to simulate a series of numbers according to FRF measurements. In order to evaluate the descriptive method in controlled condition, the researcher presupposed that the collected data from measurements are free from any noise. In addition, this work reveals that the Prediction approach is useful enough for noise-free data, while small errors in the analysis of measured modal FRFs negatively impact on the accuracy of the prediction of specific left axis.

In the next step, the motor of a wind turbine was used in order to be detected for its dynamic properties, while this time the data to be analyzed was taken during the motors performance. This test was designed to a) check the system when it is continuous and includes indefinite degrees of freedom b) check the measured response data when they are influenced by noise. The effect of near moods on the accuracy of the approach, and also the selection of the most optimized degree of freedom for measurement are discussed in this paper.

4. Numerical Model of Rigid Rotor with Four Degrees of Freedom

Fig 1. illustrates the tested rotor in this approach. This rotor includes a rigid Shaft, which is singed from both of its poles by two rigid disks. As it is shown in Fig 1 the disks are on the flexible and damping supports. The density of rotor is supposed to be the same as steel density, while its rotation speed is 3000 round per minute in a clock-wise direction. The left support is non-isotropic, but its anisotropic stiffness according to orthogonal coordinates system (defined through x1 and x2) is symmetric. The stuffiness matrix corresponding support is shown as below:

$$[\mathrm{K_A}] = \begin{bmatrix} 1.100 & 0.100 \\ 0.100 & 1.100 \end{bmatrix} \times 10^5 \quad \frac{\mathrm{N}}{\mathrm{M}} \tag{7}$$

The right support contains a non-symmetric anisotropic stiffness, which acts like a hydrodynamic bearing. The stuffiness matrix of this support according to orthogonal coordinate system shown via x3 and x4 is as below:

$$[\mathrm{K_B}] = \begin{bmatrix} 1.100 & 0.124 \\ 0.076 & 1.100 \end{bmatrix} \times 10^5 \quad \frac{\mathrm{N}}{\mathrm{M}} \tag{8}$$

During the rotation time, gyroscopic forces are produced. This phenomenon is because of the combination of angular momentum effects of the disk around rotation axis on the one hand, and also this axis’s deviation on the other hand. These effects result in the emergence of a section in damping matrix system, which is known as the symmetric-antithetic component.

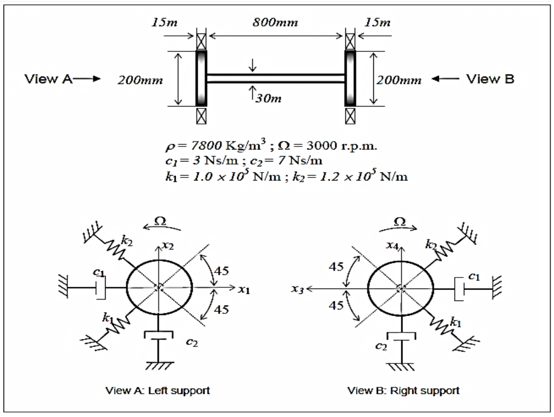

Fig. 1. Rigid rotor with four degrees of freedom

Degrees of freedom in this analysis are x_1, x_2, x_3 and x_4, whereby the rotor’s movement is defined according to their movements (figure 1). The Mass, stuffiness and damping matrixes corresponding to these degrees of freedom are defined as below:

$$[\mathrm{M}] = \begin{bmatrix} 5.161 & 0 & 0.720 & 0 \\ 0 & 5.161 & 0 & 0.720 \\ 0.720 & 0 & 5.161 & 0 \\ 0 & 0.720 & 0 & 5.161 \end{bmatrix} \mathrm{Kg} \tag{9}$$

$$[C] = \begin{bmatrix} 3.000 & 17.620 & 0 & -17.620 \\ -17.620 & 7.000 & 17.62 & 0 \\ 0 & -17.620 & 3.00 & 17.620 \\ 17.620 & 0 & -17.62 & 7.000 \end{bmatrix} \frac{N}{M/S} \tag{10}$$

$$[\mathrm{K}] = \begin{bmatrix} 1.100 & 0.100 & 0 & 0 \\ 0.100 & 1.100 & 0 & 0 \\ 0 & 0 & 1.100 & 0.124 \\ 0 & 0 & 0.076 & 1.100 \end{bmatrix} \times 10^5 \ \frac{\mathrm{N}}{\mathrm{M}} \tag{11}$$

The system size is N=4. In equations (10) and (11) it is clear that the number of degrees of freedom dealt with non-symmetric sections of stuffiness and damping matrixes –shown with dotted line- are n_k=2 and n_c=4 in respect. According to the explained suppositions in properties Prediction approach, matrix is the symmetric mass. Below, the procedure of the determination of the system specific left axis through the simulated measurements of FRF is discussed.

ISSN: 2251-9246
EISSN: 2345-6221

5. Required FRFs

According to the equations (12), (13) and (14) the complete identification of the system requires the measurement of a full column of FRF matrix and at least two components of one of its rows. The occurrence of such condition provides the situation for the co-occurrence of below equations.

$$q \geq 1 \tag{12}$$

$$q \geq \sqrt{n_c^2 + n_k^2} - N + 1 = 1.4721 \tag{13}$$

$$q \geq \max\,(n_c, n_k) - 2[N - min(n_c, n_k)] = 0 \tag{14}$$

The FRFs' of corresponding rush to the first column of FRF matrix and an extra FRF from the first row are shown in (figure 2). What is explained in this figure is called measured FRFs, because they exactly play the role of real measured FRFs in the identification of a real system.

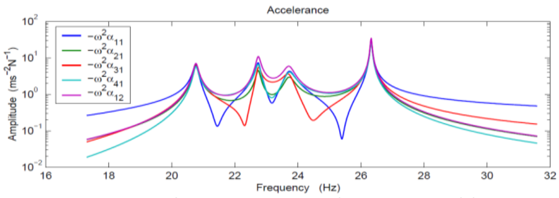

Fig. 2. FRFs of a rigid rotor with four degrees of freedom

6. FRF Data Modal Analysis

From modal analysis of measured FRF data some natural frequencies, damping coefficient and also fixed modal amounts could be identified. For studying such a system, at first, simulation is done through MATLAB software and then the provided data are analyzed there too. Natural frequencies and damping coefficient were identified through least squares method (table 1). In Table 2. the estimated modal fixed amounts for the full series of measured FRFs are shown. In the prediction of the specific left axis it is very important to keep in mind that the estimated modal fixed amounts corresponding a system's model is through damping hysteric mood, while Prediction approach for a system is applied through viscose damping mood. Hence, it is necessary to identify a series of modal parameters that are in harmony with viscose damping system, before the estimation of specific left axis in this approach. If suppose that damping, viscose, and hysteric coefficients are fixed and equal to their amounts in resonance, the natural damping frequencies ϖ_r, critical damping ratio ζ_r, complex fixed amounts λ_r, in a system with viscose damping, will be related to the natural frequencies ω_r, and damping coefficient η_r, in system with hysteric damping; according to below formulas and relations.

$$\varpi_r = \omega_r \sqrt{1 - \frac{\eta_r^2}{4}} \tag{15}$$

$$\zeta_r = \frac{\eta_r}{2} \tag{16}$$

$$\lambda_r = -\zeta_r \omega_r + i\varpi_r \tag{17}$$

Natural frequencies, critical damping coefficient, and complex fixed amounts in a system with viscose damping corresponding to their equals that were shown in Table 1, are provided in Table 3.

Table.1.
Natural frequencies and estimated hysteric damping coefficient

MODE, r	ω_r ***(Hz)***	n_r
1	20.7650	0.0065
2	22.7429	0.0059
3	23.4181	0.0133
4	26.3260	0.0017

Table.2.
Estimated damping fixed amounts for a hysteric damping modal

FRF	***MODE1***	***MODE2***
$-\omega^2\alpha_{11}$	0.0063-0.1638i	0.0043-0.1478i
$-\omega^2\alpha_{21}$	-0.0019 +0.1546i	0.0075-0.0965i
$-\omega^2\alpha_{31}$	0.0044-0.1725i	-0.0014 -0.1102i
$-\omega^2\alpha_{41}$	0.0000 +0.1448	0.0020-0.1320
$-\omega^2\alpha_{12}$	-0.0460 -0.0005i	0.0631 +0.0021i
FRF	***MODE3***	***MODE4***
$-\omega^2\alpha_{11}$	-0.0079 -0.1851i	-0.0005 -0.1736i
$-\omega^2\alpha_{21}$	0.0714 +0.1175i	-0.0792 -0.1433i
$-\omega^2\alpha_{31}$	-0.0088 +0.1519i	0.0045 +0.1786i
$-\omega^2\alpha_{41}$	-0.0797 -0.1514i	0.0798 +0.1357i
$-\omega^2\alpha_{12}$	-0.0689 -0.0304i	0.0516 +0.320i

Table.3.
Natural frequencies and estimated critical viscose damping ratio

MODE, r	ω_r ***(Hz)***		λ_r
1	20.7649	0.0033	-0.4255+130.47i
2	22.7428	0.0029	-0.4185+142.90i
3	23.7176	0.0066	-0.9889+149.02i
4	26.3260	0.0008	-0.1406+165.41i

In order to check the accuracy and scrutiny of the resulted parameters with a reference, their exact amounts were directly measured through space-featured matrixes written in equations 9 to 11. In the error column, the difference between exact and estimated amounts is exhibited in the form a percent of their exact amounts.

7. Normalization of Specific Axis

The estimated modal fixed amounts are used in order to extract the normalized specific right axis and two components of the normalized specific left axis. Normalization helps to define an optimal amount for a component from specific right or left axis in any mood. Nonetheless, through the below relationship, it is possible to relate modal fixed amounts to corresponding elements in normalized specific right or left axis for each FRF .

$$ {}_{r}A_{ij} = (\varphi_R)_{ri}(\varphi_L)_{rj} \tag{18} $$

In this relationship r indicates the number of mood, i and j describe the number of row and column of FRF matrix, which agree their measured FRFs.

It is supposed that the elements of measured FRF are equal in all of the moods.

$$ (\varphi_R)_{r1} = (\varphi_L)_{r1} = \sqrt{{}_{r}A_{11}} \tag{19} $$

Also, the elements of specific left axis could be evaluated via using the suitable index of j in below formula:

$$ (\varphi_L)_{rj} = \frac{{}_{r}A_{1j}}{{}_{r}A_{11}} \cdot (\varphi_L)_{r1} \tag{20} $$

Using equations (19) and (20), and estimated modal fixed amounts (table 4); it is possible to identify normalized specific right axis and two elements of each normalized specific left axis. These amounts are provided in table 5.

8. Simulation Results

In this system and for the sake of simplicity, the normalized specific right and left axis are named as specific left and right axis in brief. After the identification of specific amounts, specific axis and two elements each specific left axis from measured FRF, the calculation of other elements of specific left axis through a system of equations become possible. In order to evaluate the accuracy of measured elements, exact fixed modal amounts were measured directly via space-featured matrixes in equations (3) to (5). The estimated specific left axis in table 6 was compared to their counterparts. In the error column, the difference between exact and estimated amounts is exhibited in the form a percent of their exact amounts.

9. Conclusion and Discussion

In the studied system, specific left axis of the shown rotor in Fig 1. to Fig 5. were identified through the measurement of a column of FRF matrix and an extra element of a row. It was shown that how measuring the modal parameters of an orbital machine structure through the measurement of a column of FRF matrix and all of its rows become possible. In addition, the results in table 6 indicate that the prediction of specific left axis with the accuracy of 98% is viable, which is higher than what was provided in the analysis of the real measured data. The results of this paper revealed that Prediction approach can help in the exact estimation of specific left axis. However, the impact of natural factors like noise in the measured data or the accuracy of estimated modal parameters were disregarded.

Table.4.
Comparison of *1ooo modal fixed amounts for a system with viscose damping

M	*FRF*	*EXACT*	*ESTIMATED*	*ER %*
1	–	0.0060-0.1649i	0.0063-0.1638i	0.6910
	–	-0.0015+0.1544i	-0.002+0.1546i	0.2896
	–	0.0041-0.1724i	0.0044-0.1725i	0.1834
	–	0.0002+0.1441i	0.0000+0.1448i	0.5052
	–	-0.0019+0.1763i	-0.002+0.1763i	0.0000
2	–	0.0031-0.11471i	0.0043-0.1478i	0.9442
	–	0.0081-0.0973i	0.0075-0.0965i	1.0242
	–	-0.0018-0.1110i	-0.0014-0.1102i	0.8057
	–	0.0003-0.1311i	0.0020-0.1320i	1.4672
	–	0.0047-0.2218i	0.0073-0.2208i	1.2557

Table.5.
The normalized estimated specific right and left axis elements

FRF	*MODE1*	*MODE2*
$\{\Phi_R\}_r$	0.0092-0.0089i	0.0087+0.0085i
	-0.0085+0.0086i	0.0060-0.0053i
	0.0096-0.0095i	0.0062-0.0066i
	-0.0078+0.0081i	0.0077-0.0077i
	0.0092-0.0089i	0.0087-0.0085i
	-0.0097+0.0098i	0.0131-0.0126i
FRF	***MODE3***	***MODE4***
$\{\Phi_R\}_r$	0.0094-0.0098i	0.0093-0.0093i
	-0.0026+0.0098i	0.0035-0..0119i
	-0.0085+0.0073i	-0.0094+0.0098i
	0.0040-0.0119i	-0.0030+0.0116i
	0.0094-0.0098i	0.0093-0.0093i
	-0.0175+0.0064i	0.0136-0.0032i

Errors explained in table 6 would stem from three types of sources: the first type is limiting the quantities of the calculations to only four numbers, which in contradiction to large amounts, may cause problems and errors during the calculation of small amounts.

The second type refers to the process of identification of specific amounts and modal fixed amounts of measured FRF. The accuracy of identification of these parameters depends on different selections that are done via analysis of their modals like the selection of curve-fitting algorithm or selection of the dots used for practice. The selections depend largely on human capabilities and talents, and this factor may cause many errors in the estimations.

The third type, which may be the most important one, might come from the wrong selection of algorithm, whereby an algorithm that may suit the systems with viscose damping is used for the system with hysteric damping erroneously.

Although in limited frequency spaces like resonance areas, a viscose damping system's treatment would be modelled to a hysteric damping system, but the remarkable differences between these two may not be disregarded in real model and supposed model.

Beside the mentioned numerical errors, actual factors such as noise, selection of degrees of freedom for provocation of structure, and selection of degrees of freedom for measuring the structure responses to the provocations may impact on the accuracy of modal parameters.

Table.6.
Comparison of specific left axis

M	***EXACT***	***ESTIMATED***	***ER %***
1	0.0092-0.0089i	0.0092-0.0089i	0.0000
	-0.0096 +0.0098i	-0.0097 +0.0098i	0.7289
	0.0086-0.0084i	0.0086-0.0085i	0.8318
	-0.0100 +0.0103i	-0.0100 +0.104i	0.6966
2	0.0087-0.0085i	0.0088-0.0084i	1.1627
	0.0131-0.0128i	0.0131-0.0126i	1.0920
	0.0109-0.0121i	0.0109-0.0118i	1.8421
	0.0096-0.0099i	0.0098-0.0098i	1.6215
3	0.0094-0.0098i	0.0094-0.0099i	0.7364
	-0.0174 +0.0065i	-0.0175 +0.0064i	0.7614
	-0.0124 +0.0117i	-0.0124 +0.0115i	1.1731
	0.0145-0.0041i	0.0147-0.0043i	1.8770
4	0.0093-0.0093i	0.0093-0.0093i	0.0000
	0.0136-0.0031i	0.0136-0.0032i	0.7169
	-0.0087 +0.0092i	-0/0087 +0.0094i	1.5795
	-0.0139 +0.0036i	-0.0139 +0.0037i	0.6964

Reference

[1] S. Cornelius, and P. Girdhar, "Practical machinery vibration analysis and predictive maintenance", Newnes, 2004.

[2] Y. Han, and Y. H. Song. "Condition monitoring techniques for electrical equipment-a literature survey", IEEE Transactions on Power Delivery, vol.18, no.1 , 2003.

[3] S.A. Mortazavizadeh, A. Vahedi and A. Zohouri, "Detection of Stator Winding Inter-turn Short Circuit In Induction Motor Using Vibration Specified Harmonic Amplitude", 2nd International Conf. on Acoustics & Vibration, Sharif Univ. of Technology, Tehran, Iran, Dec. 2012.

[4] S. Pöyhönen, "Numerical magnetic field analysis and signal processing for fault diagnostics of electrical machines", COMPEL: The International Journal for Computation and Mathematics in Electrical and Electronic Engineering , vol.22, no.4, 2003.

[5] C. Seungdeog, "Performance-oriented electric motors diagnostics in modern energy conversion systems", IEEE Transactions on Industrial Electronics, vol.59, no.2, 2012.

[6] D.G. Dorrell, T.William and S. Roach. "Analysis of airgap flux, current, and vibration signals as a function of the combination of static and dynamic airgap eccentricity in 3-phase induction motors", IEEE Transactions on Industry Applications,vol.33, vol.1 ,1997.

[7] J. Zhuge, " Vibration Data Collector Signal Analysis", Part of VDC User's Manual, CRYSTAL instrument, 2009.

[8] W. Finley, M. Hodowanec, and W.G. Holter. "An analytical approach to solving motor vibration problems." Petroleum and Chemical Industry Conference, Industry Applications Society 46th Annual. IEEE, 1999.

[9] J.R. Cameron, W. T. Thomson, and A. B. Dow. "Vibration and current monitoring for detecting airgap eccentricity in large induction motors", IEE Proceedings Electric Power Applications, vol.133, no. 3, 1986.

[10] Rodríguez, Pedro Vicente Jover, et al. "Air-gap force distribution and vibration pattern of induction motors under dynamic eccentricity", Electrical Engineering ,vol.90, no.3 ,2003.

[11] Ellison, A. J., and S. J. Yang. "Effects of rotor eccentricity on acoustic noise from induction machines", Proceedings of the Institution of Electrical Engineers. vol. 118, no. 1. IET Digital Library, 1971.

[12] Li, Ruoyu, and David He. "Rotational Machine Health Monitoring and Fault Detection Using EMD-Based Acoustic Emission Feature Quantification", Instrumentation and Measurement, IEEE Transactions on vol.61, no.4 , 2012.

[13] N. Baydar, and A. Ball. "A comparative study of acoustic and vibration signals in detection of gear failures using Wigner–Ville distribution", Mechanical Systems and Signal Processing", vol.15, no.6 , 2001.

[14] L. Meirovitch, "A new method for the solution of the eigenvalue problem for gyroscopic systems", AIAA Journal, vol. 12, no.10, 1974.